JDI Journal of Diabetes Investigation Open access
Official Journal of the Asian Association for the Study of Diabetes
ORIGINAL ARTICLE

miR-4431 targets TRIP10/PRKD1 and impairs glucose metabolism

Chongge Pan[1†], Menghuan Li[2†], Jingzhou Wang[1], Xiaolong Chu[1], Jianyu Xiong[1], Xin Yang[1], Yihan Tang[1], Dingling Ma[1], Chenggang Yuan[1], Jiaojiao Zhu[1], Yongsheng Chang[2,3], Jun Zhang[1], Cuizhe Wang[4*]

[1]Department of Biochemistry and Molecular Biology, Shihezi University School of Medicine, Shihezi, China, [2]Shihezi University School of Medicine, Shihezi, China, [3]Department of Physiology and Pathophysiology, Tianjin Medical University, Tianjin, China, and [4]Ministry of Education Key Laboratory of Xinjiang Endemic and Ethnic Disease, Shihezi, China

Keywords
miR-4431, Glucose metabolism, Type 2 diabetes mellitus

***Correspondence**
Cuizhe Wang
Tel.: +86-0993-2055801
Fax: +86-0993-2055801
E-mail address:
wangcuizhe905@163.com

J Diabetes Investig 2022; 13: 617–627

doi: 10.1111/jdi.13714

ABSTRACT

Aim/Introduction: Obesity is considered an important risk factor for many metabolic disorders, especially type 2 diabetes mellitus, and microRNAs (miRNAs) play a vital role in the development of type 2 diabetes mellitus. Therefore, we conducted this study to investigate the role of miR-4431 in the obesity-associated pathobiology of type 2 diabetes mellitus.

Materials and methods: Subjects were divided into normal control (n = 36), obese (n = 36), and type 2 diabetes mellitus (n = 12) groups, and serum miR-4431 levels were analyzed. Adenovirus-vectored miR-4431 mimic or sponge was intraperitoneally injected into the normal diet group and the high-fat diet group (HFD) mice to investigate glucose tolerance, insulin sensitivity, and lipid levels. The downstream target genes of miR-4431 were predicted using bioinformatics, and they were verified *in vitro*.

Results: Serum miR-4431 levels were significantly high in obese and type 2 diabetes mellitus individuals, and positively correlated with the body mass index and fasting plasma glucose levels. In HFD mice, miR-4431 levels in the serum, white adipose tissue, and liver were significantly increased. Moreover, miR-4431 impaired glucose tolerance, insulin sensitivity, and lipid metabolism in mice. Bioinformatic prediction suggested that TRIP10 and PRKD1 could be the downstream target genes of miR-4431. The HFD mice showed a remarkable reduction in the mRNA levels of TRIP10 and PRKD1 in the liver, which were countered by blocking miR-4431. In HepG2 and L02 cells, miR-4431 could downregulate TRIP10 and PRKD1 while blocking glucose uptake. The luciferase reporter assay showed that miR-4431 could bind TRIP10 and PRKD1 3′-UTR.

Conclusion: miR-4431 targets TRIP10/PRKD1 and impairs glucose metabolism.

INTRODUCTION

Since 1980, the prevalence of overweight and obesity has doubled globally, and approximately one-third of the population is now classified as overweight or obese[1]. Obesity is considered an important risk factor for many metabolic disorders, especially type 2 diabetes mellitus. According to epidemiological data, in 80% of patients, type 2 diabetes mellitus is caused by obesity[2,3]. However, the specific mechanism is not yet fully understood.

Obesity is characterized by an excessive accumulation of adipose tissue, especially white adipose tissue, which not only stores energy from the diet but also releases metabolic agents, such as microRNAs (miRNAs, miR), that are involved in regulating energy homeostasis[4]. miRNAs are small, non-coding, 21–23 nucleotide-long RNAs that can negatively regulate gene expression by pairing with the 3′-untranslated region (3′ UTR) of specific mRNAs[5]. In recent years, studies have investigated the role of miRNAs in the regulation of obesity and glucose metabolism.

It has been reported that obesity-induced miR-101, miR-375, and miR-802 are biomarkers of type 2 diabetes mellitus[6,7]. Circulating miR-122 is strongly associated with the risk of developing metabolic syndrome and type 2 diabetes mellitus[8]. Moreover, obesity-associated microRNAs, such as miR-192, miR-27a-3p, and miR-27b-3p, can modulate glucose and lipid metabolism in mice[9]. Recent studies have demonstrated that miR-155 and miR-29 levels are elevated in the serum of obese and type 2 diabetes mellitus patients, and an overexpression of miR-155 and miR-29 in HepG2 cells negatively impacts glucose and lipid metabolism[10]. These results suggest the important role

†Equal contribution.

Received 31 August 2021; revised 8 November 2021; accepted 15 November 2021

of miRNAs in obesity and related metabolic disorders. Therefore, investigation of differentially expressed miRNAs will provide new ideas for the personalized treatment of obesity and type 2 diabetes mellitus.

Our previous unpublished single nucleotide polymorphism (SNP) microarray of blood samples from 1,053 subjects screened out miR-4431, which was significantly related to fasting plasma glucose (FPG), high-density lipoprotein cholesterol (HDL-C), low-density lipoprotein cholesterol (LDL-C), triglyceride (TG), and total cholesterol (TC). However, the function of miR-4431 has not been reported to date. To better understand the role of miR-4431 in the obesity-associated development of type 2 diabetes mellitus, in this study, we analyzed serum miR-4431 levels in normal control, obesity, and type 2 diabetes mellitus individuals. Moreover, we intraperitoneally injected adenovirus-vectored miR-4431 mimic or sponge into normal diet group (ND) and high-fat diet group (HFD) mice to determine the effect of miR-4431 on glucose and lipid metabolism.

METHODS

Subjects

Serum samples from 36 normal control subjects, 36 obese individuals, and 12 type 2 diabetes mellitus individuals were collected from 51 regiment hospital in Xinjiang, China from July to August 2019. General data such as age, height, weight, body mass index (BMI), and waist circumference (WC) were gathered, and biochemical indexes such as FPG, TG, TC, HDL-C, and LDL-C were detected. Individuals between 40 and 60 years of age were included in the study. Additionally, the inclusion criteria for normal control individuals were $18.5\ kg/m^2 \leq BMI < 28\ kg/m^2$ and $FPG < 6.1$ mmol/L; those for obese individuals were $BMI \geq 28\ kg/m^2$ and $FPG < 6.1$ mmol/L; and those for type 2 diabetes mellitus individuals were plasma glucose ≥ 11.1 mmol/L at 2 h postprandial and $FPG \geq 7.0$ mmol/L. The ratio of males to females was 1:1. The exclusion criteria were as follows: (1) for normal control and obese individuals: individuals with diabetes, hypertension, cancer, other metabolic diseases, and no history of taking drugs; (2) for individuals with type 2 diabetes mellitus: diagnosis for the first time and no history of taking hypoglycemic and lipid-lowering drugs previously. The diagnostic criteria for type 2 diabetes mellitus were based on the WHO criteria issued in 1999.

Adenovirus constructs

The miR-4431 mimic adenovirus and miR-4431 sponge adenovirus used in animal experiments were purchased from Jima Pharmaceutical Technology Co., Ltd, Shanghai, China. The adenovirus was amplified from 293A cells. When the cells grew to approximately 50% confluence, the 293A cells were added to the adenovirus seed. After culturing for 2–3 days, a cytopathic effect (CPE) was observed. Following this, adenovirus stock was harvested through repeated freezing and thawing, and it was purified using the ViraTrap™ Adenovirus Purification Miniprep Kit (Biomiga, San Diego, USA).

Animal experiment

Male C57BL/6 mice aged 4–6 weeks were purchased from Hunan SJA Laboratory Animal Co., Ltd, Hunan, China, and they were raised in the Experimental Animal Center of Shihezi University School of Medicine. The animal room guaranteed a constant-temperature environment and 12:12 h light/dark cycle. Mice had free access to food and water. After 1 week of adaptive feeding, the mice were divided into ND ($n = 22$) and HFD groups ($n = 22$), and their body weight was dynamically monitored. After feeding for 16 weeks, six ND mice and six HFD mice were euthanized, and white adipose tissue (WAT), serum, and liver were collected to analyze the expression level of miR-4431. Following this, 16 ND mice were intraperitoneally injected with adenovirus-vectored NC mimic or miR-4431 mimic ($n = 8$, $1*10^{11}$VP/mouse, once a week) for 6 weeks. Additionally, another 16 HFD mice were intraperitoneally injected with adenovirus-vectored NC sponge and miR-4431 sponge ($n = 8$, $1*10^{11}$VP/mouse, once a week) for 6 weeks. The miR-4431 mimic adenovirus and miR-4431 inhibitor vector adenovirus used in the animal experiments were purchased from Shanghai Jima Pharmaceutical Technology Co., Ltd. Thus, the mice were divided into four groups, i.e., ND + NC mimic group ($n = 8$), ND + miR-4431 mimic group ($n = 8$), HFD + NC sponge group ($n = 8$), and HFD + miR-4431 sponge group ($n = 8$).

In week 22, the glucose tolerance and insulin sensitivity of mice were evaluated using an intraperitoneal glucose tolerance trial (GTT) and insulin tolerance test (ITT). Fundus vein blood was collected to detect the lipid and glucose contents. The liver and adipose tissues, such as brown adipose tissue (BAT), epididymal WAT (eWAT), subcutaneous WAT (subWAT), perinephric WAT (pWAT), and visceral WAT (vWAT), were weighed, and they were immediately stored at −80°C for further analysis.

Serum biochemical indexes test

Serum FFA, TC, TG, HDL-C, and LDL-C test kits were purchased from the Nanjing Jiancheng Institute of Bioengineering, Nanjing, China. Roche blood glucose test strips and a Roche blood glucose meter (Roche Blood Glucose Health Medical Care Company, Shanghai, China) were used for blood glucose testing in mice.

GTT and ITT

For the GTT, A 20% glucose solution was prepared with normal saline and D-glucose (CAT# G6125, Sigma-Aldrich, St Louis, Missouri, USA). After fasting for 16 h, blood was collected from the tail of mice to measure fasting blood glucose level, and the measured value was recorded as the blood glucose value at 0 min. Each mouse was intraperitoneally injected with glucose solution at a dose of 2 g/kg. The blood glucose levels of each mouse were measured at 15 min, 30 min, 60 min, 90 min, and 120 min.

For the ITT, The dosage of insulin was 0.5 U/kg, and insulin (Novoline 30R) was diluted with normal saline to prepare a solution with a concentration of 0.5 U/mL. The mice were

allowed to fast for 4–6 h, and water was then administered normally. The blood glucose level was measured before insulin injection, and the blood glucose level of each mouse was measured at 15 min, 30 min, 60 min, 90 min, and 120 min after insulin injection.

Cell culture

The HepG2 and HEK-293T cell lines used in this study were purchased from the Cell Bank of Treasures Committee of Typical Cultures, Chinese Academy of Sciences, Beijing, China. The L02 and 293A cells were purchased from Shanghai OE Biotech. Co. Ltd, Shanghai, China, and the cells were cultured in high glucose Dulbecco's modified Eagle's medium (DMEM, Gibco, California, USA) + 10% fetal bovine serum (FBS, Biological Industries, Kibbutz Beit Haemek, Israel) + 1% penicillin-streptomycin (solarbio, Beijing, China) at 37°C in a 5% CO_2 atmosphere.

Transfection of miR-4431 mimic/inhibitor

The miR-4431 mimic/inhibitor and negative control (NC) mimic/inhibitor required for cell transfection were synthesized by Gene Pharma Company (Shanghai, China), and they were then dissolved in diethyl pyrocarbonate (DEPC, solarbio, Beijing, China) water after centrifugation for later use. The miR-4431 mimic (70 nmol/L) and inhibitor (100 nmol/L) were mixed with Lipofectamine 2000 (cat# 11668-019; Invitrogen, California, USA), incubated at room temperature for 20 min, added into a six-well plate containing cells and DMEM, and cultured in a 5% CO2 incubator at 37°C. The solution was changed after 4 h, and RNA was extracted after 24 h.

RNA isolation and quantitative real-time PCR (qRT-PCR)

miR-4431 was extracted using the miRcute miRNA isolation kit (cat# DP503; TianGen, Beijing, China). The miRcute Plus microRNA first strand cDNA kit (cat# KR211; TianGen, Beijing, China) was used for reverse transcription of miRNA first chain cDNA, and the miRcute Plus microRNA SYBR Green qPCR Kit (cat# FP401; TianGen) was used to detect the expression of microRNA. U6 was used as an internal reference to calculate the relative expression of miR-4431. The hsa-miR-4431 sequence is presented in Table S1.

Total RNA was extracted from cells using TRIZOL reagent (cat# 15596-026; Life Technologies, California, USA), and reverse transcription was performed at 42°C for 60 min and then at 70°C for 15 min. PCR amplification was performed using a qRT-PCR instrument (Qiagen, Hilden, Germany) with the following program settings: 95°C for 3–5 min, 40–45 cycles at 95°C for 10 s, 50–60°C for 30 s, and 72°C for 40 s. GAPDH was used for standardization. The primer sequences are listed in Table S2.

Western blot

The proteins were extracted from cells using the RIPA lysis buffer. The extracted proteins were electrophoresed and transferred to membranes. Then, the membrane was blocked with 5% fat-free milk for 2 hours, and subsequently incubated with primary antibody (1:1000 ratio) at 4°C overnight. The membrane was washed 3 times with Tris-Buffered Saline Tween-20 buffer, and treated with secondary antibody (1:10000 ratio) for 2 hours at room temperature. The protein level was detected with enhanced chemi-luminescence system (Pierce Biotechnology Inc., California, USA). The primary antibodies: anti-β-Tubulin 55kDa (Zhongshan Jinqiao, Beijing, China), anti-TRIP10 68 kDa (Abcam, Massachusetts, USA), anti-PRKD1 102 kDa (Abcam, Massachusetts, USA).

Glucose content test

The HepG2 and L02 cells were starved using FBS-free DMEM medium for 12 h, and they were then transfected with an miR-4431 mimic or inhibitor for 24 h, respectively. The glucose oxidase method (CAT# F006; Nanjing JianCheng Biological Engineering Research Institute) was used to determine the glucose concentration in the cell supernatant.

Luciferase reporter assay

The HEK-293T cells were transfected with a firefly luciferase vector encoding TRIP10 (TRIP10-WT) or PRKD1(PRKD1-WT) 3′UTR, firefly luciferase vector encoding the mutant TRIP10 (TRIP10-Mut) or PRKD1 (PRKD1-Mut) 3′UTR, Renilla luciferase vector (Gene Pharma Company, Shanghai, China), and miR-4431 mimic or NC mimic using Lipofectamine 3000® Transfection Reagent (Invitrogen). After 24 h, luminescence was determined using the Dual-glo-luciferase-assay-system (CAT# REFE2920; Promega, Wisconsin, USA). The luminescence results were normalized to the Renilla luminescent signal.

Statistical analysis

SPSS17.0 (SPSS Inc., Chicago, IL, USA) was used for data analysis. The two groups of measurement data that conformed to the normal distribution and variances were tested using an unpaired Student's *t*-test, and the non-parametric rank-sum test was used to compare the two groups of data inconsistent with normal distribution. Pearson correlation coefficient was used to analyze linear correlations between the two variables. Statistical significance was set at $P < 0.05$. Data are expressed as mean ± SD or mean ± SEM.

RESULTS

Serum miR-4431 was significantly overexpressed in obese and type 2 diabetes mellitus individuals, and it was positively correlated with BMI and FPG

To determine the correlation between miR-4431 and the development of obesity and type 2 diabetes mellitus, we detected serum miR-4431 levels in 36 NC individuals, 36 obese individuals, and 12 individuals with type 2 diabetes mellitus. Table 1 shows the general data, biochemical indexes, and serum miR-4431 levels of subjects. Figure S1 shows the data dispersion.

Table 1 | General data, biochemical indexes, and serum miR-4431 expression of individuals

Indexes	NC	Obese	Type 2 diabetes mellitus
n	36	36	12
Age (years)	40.00 ± 13.54	52.05 ± 13.74*	56.00 ± 12.10*
Height (cm)	166.00 ± 10.18	160.91 ± 7.7*	160.91 ± 10.29
Weight (kg)	66.25 ± 10.82	81.10 ± 9.22*	80.99 ± 11.10*
BMI (kg/m^2)	24.03 ± 3.13	31.33 ± 3.07*	31.55 ± 5.47*
WC (cm)	84.08 ± 10.18	102.44 ± 9.89*	104.58 ± 12.21*
FPG (mmol/L)	4.30 ± 0.54	4.68 ± 0.66	10.13 ± 3.01*,#
TG (mmol/L)	1.28 ± 0.78	2.16 ± 1.07*	3.97 ± 3.47*,#
TC (mmol/L)	4.60 ± 1.25	5.09 ± 0.91	5.57 ± 1.63*
LDL-C (mmol/L)	2.27 ± 0.91	2.45 ± 0.62	2.60 ± 0.93
HDL-C (mmol/L)	2.01 ± 0.61	2.06 ± 0.45	2.21 ± 0.65
miR-4431	0.0135 ± 0.0149	0.0612 ± 0.1035*	0.0664 ± 0.0750*

Values are presented by mean ± SD. Nonparametric rank sum test, *$P < 0.05$, compared with the normal control group; #$P < 0.05$, compared with the obese group, the difference was statistically significant. BMI, body mass index; FPG, fasting plasma glucose; HDL-C, high-density lipoprotein cholesterol; LDL-C, low-density lipoprotein cholesterol; TC, total cholesterol; TG, triglycerides; WC, waist circumference.

Our results showed that the weight, BMI, WC, and TG of obese individuals were significantly higher than those of the NC group ($P < 0.05$, Table 1). Moreover, the body weight, BMI, WC, FPG, TG, and TC of type 2 diabetes mellitus individuals were significantly higher than those of NC individuals ($P < 0.05$, Table 1). Additionally, compared with obese individuals, the FPG and TG of type 2 diabetes mellitus individuals were significantly higher ($P < 0.05$, Table 1). Following this, miR-4431 levels in human serum samples were detected using qRT-PCR, and the results showed that miR-4431 expression was significantly higher in obese and type 2 diabetes mellitus groups compared with that in the NC group ($P < 0.05$, Table 1). Correlation analysis between serum miR-4431 expression levels and general data demonstrated that serum miR-4431 expression levels were positively correlated with BMI and FPG ($P < 0.05$, Figure 1).

miR-4431 impairs glucose and lipid metabolism in mice

To determine the effect of miR-4431 on glucose and lipid metabolism *in vivo*, the mice were fed HFD or ND for 16 weeks. The results showed that the weight gain of HFD mice was significantly higher than that of ND mice ($P < 0.01$, Figure 2a). Moreover, in contrast to ND mice, miR-4431 expression was elevated in the serum, WAT, and liver of HFD mice ($P < 0.05$, Figure 2g). Interestingly, the miR-4431 level in the liver was over 10-fold higher than that in the serum and WAT (Figure 2g), suggesting that the main target tissue of miR-4431 was probably the liver.

Following this, we intraperitoneally injected an adenovirus-vectored miR-4431 mimic or sponge into ND and HFD mice. Our results showed that miR-4431 had no effect on the body weight and adipose tissue weights, such as eWAT, subWAT, pWAT, and vWAT (Figure 2a–c). Compared with those in the ND + NC mimic group, serum levels of FFA, TC, TG, HDL-C, and GLU significantly increased in the ND + miR-4431 mimic group ($P < 0.05$, Figure 2d). Moreover, in contrast to those in the HFD + NC sponge group, the serum levels of TG, LDL-C, and GLU significantly decreased while the level of HDL-C significantly increased in the HFD + miR-4431 sponge group ($P < 0.05$, Figure 2d). More importantly, GTT and ITT experiments showed that glucose tolerance and insulin sensitivity were significantly reduced in the ND + miR-4431 mimic group compared with those in the ND + NC mimic group ($P < 0.01$, Figure 2e,f). In contrast, the HFD + miR-4431 sponge mice exhibited a significant improvement in glucose tolerance and insulin sensitivity compared with the HFD+NC sponge group ($P < 0.01$, Figure 2e,f). These results demonstrated that miR-4431 impaired glucose and lipid metabolism in mice.

TRIP10 and PRKD1 can be the downstream target genes of miR-4431

We used TargetScan software (http://www.targetscan.org/vert_72/) and miRDB (http://mirdb.org/) software to predict the potential downstream genes of miR-4431. KEGG pathway enrichment was evaluated using the Kobas software (http://kobas.cbi.pku.edu.cn/). In total, 631 genes were predicted as the downstream targets of miR-4431 using TargetScan software while only 22 genes were predicted using the miRDB software. The top 30 genes determined using TargetScan software and 22 genes with miRDB software are listed, and their KEGG pathway enrichments are presented in Tables 2 and 3. Among these genes, 10 overlapped. However, KEGG pathway enrichment showed that these 10 genes could not be involved in glucose metabolism. Notably, thyroid hormone receptor interactor 10 (TRIP10) is involved in the insulin signaling pathway. Moreover, protein kinase D1 (PRKD1) participates in the synthesis and secretion of aldosterone and rap1 signaling pathway, which

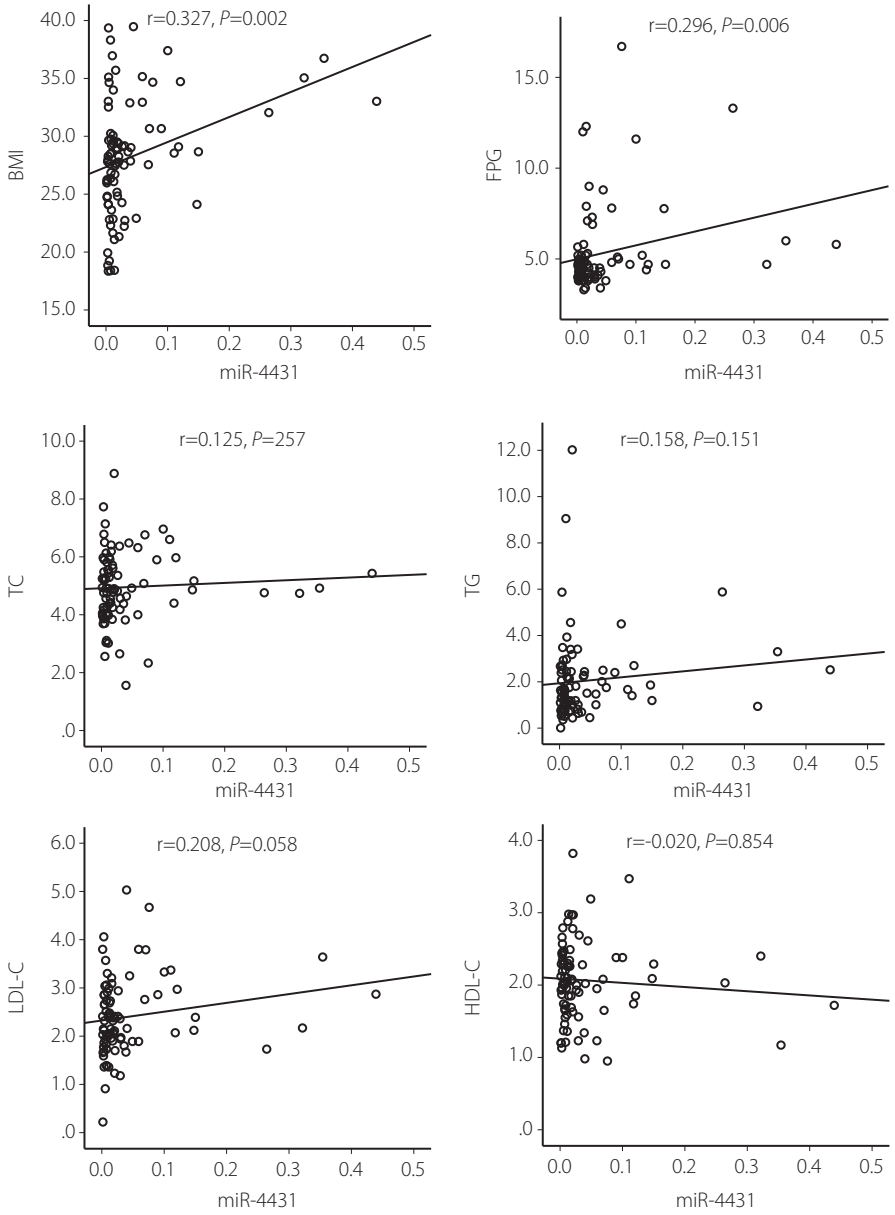

Figure 1 | Correlation analysis between miR-4431 and the general data of individuals. $n = 84$, Pearson correlation analysis. $P < 0.05$ was statistically significant.

is closely related to diabetes development[11,12]. Thus, TRIP10 and PRKD1 are downstream target genes of miR-4431.

miR-4431 inhibits the expression of TRIP10 and PRKD1 and blocks glucose uptake in hepatocytes

Next, we examined the effects of miR-4431 on TRIP10 and PRKD1 *in vivo* and *in vitro*. The results showed that HFD mice presented a significant reduction in the mRNA and protein expression levels of TRIP10 and PRKD1, which were overturned in the HFD+miR-4431 sponge mice ($P < 0.05$, Figure 2h,i,k). Interestingly, compared with the ND + NC mimic mice, the expression levels of PRKD1 significantly increased in the ND + miR-4431 mimic mice ($P < 0.01$, Figure 2h,i,j). Furthermore, to determine the effect of miR-4431 on the expression levels of TRIP10 and PRKD1 in HepG2 and L02 cells, we transfected mimic or antisense oligonucleotides (inhibitors) to overexpress or block miR-4431. Following transfection with miR-4431 mimic for 24 h, the expression levels of TRIP10 and PRKD1 were significantly decreased compared with those in the NC group in HepG2 cells ($P < 0.01$, Figure 3a,b) or L02 cells ($P < 0.01$, Figure 3d-e). Subsequently, the cell culture supernatant was collected to detect glucose content. The miR-4431 mimic significantly reduced glucose consumption in HepG2 ($P < 0.001$, Figure 2c) and L02 cells

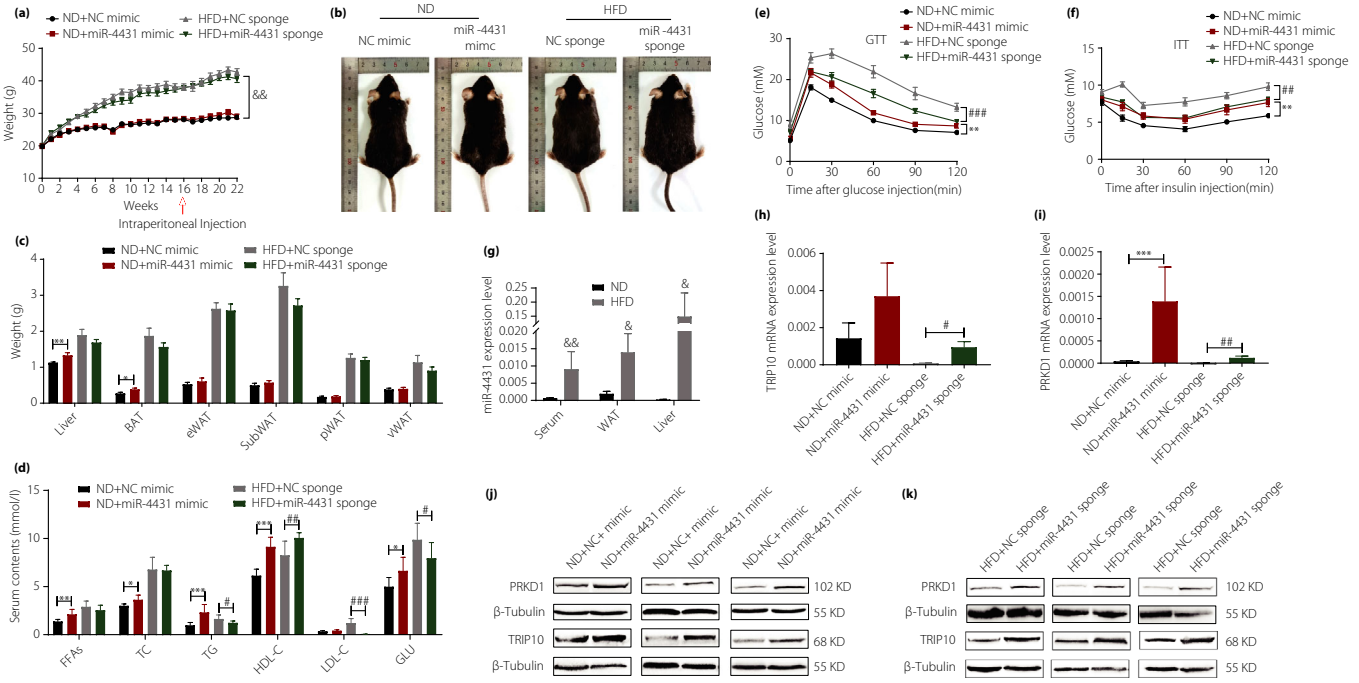

Figure 2 | Effect of miR-4431 on the glucose tolerance and insulin sensitivity of C57BL/6 mice. After feeding HFD for 16 weeks, ND and HFD mice were intraperitoneally injected with an adenovirus- vectored miR-4431 mimic or sponge (n = 8). The body weight (a, b), adipose tissues weight (c), and serum glucose and lipid levels (d) were detected (n = 8). GTT (e) and ITT (f) experiments presented glucose tolerance and insulin sensitivity of mice, respectively (n = 8). Expression levels of miR-4431 (g) in the serum, WAT, and liver in week 16 were tested (n = 6). The expression levels of TRIP10 and PRKD1 (h–k) in the liver were detected (n = 8). t-test, $^{*}P < 0.05$, $^{**}P < 0.01$, $^{***}P < 0.001$, ND + NC mimic group vs ND + miR-4431 mimic group; $^{\#}P < 0.05$, $^{\#\#}P < 0.01$, $^{\#\#\#}P < 0.001$, HFD + NC sponge group vs HFD + miR-4431 sponge group, $^{\&}P < 0.05$, $^{\&\&}P < 0.01$, ND group vs HFD group, the difference was statistically significant.

($P < 0.001$, Figure 3f). In contrast, miR-4431 inhibitor significantly increased the expression levels of TRIP10 and PRKD1 and glucose consumption in HepG2 ($P < 0.01$, Figure 3g-i) and L02 cells ($P < 0.05$, Figure 3j-l). These results suggest that miR-4431 inhibits the expression of TRIP10 and PRKD1 in hepatocytes.

miR-4431 can target the bonding between TRIP10 and PRKD1

To determine whether miR-4431 directly targeted TRIP10 and PRKD1, we constructed a luciferase reporter plasmid containing a TRIP10 or PRKD1 3′-UTR, and we tested the luciferase activity in HEK-293T cells expressing miR-4431. The results showed that miR-4431 notably repressed luciferase activity when transfected with a TRIP10-WT luciferase reporter plasmid, and the recovery of luciferase activity was observed in the mutant TRIP10 3′UTR group, indicating that miR-4431 could bind TRIP10 ($P < 0.05$, Figure 4a). Similarly, miR-4431 dramatically reduced the luciferase activity when transfected with the PRKD1-WT luciferase reporter plasmid, whereas it failed to recover luciferase activity in the mutant PRKD1 3′UTR group, suggesting the presence of other critical sequences or sites in the PRKD1 3′UTR that could bind to miR-4431 ($P < 0.05$, Figure 4b).

DISCUSSION

Recently, obesity-induced miRNAs have emerged as key regulators of abnormal glucose and lipid metabolism[13,14]. In this study, we first demonstrated a novel glucose and lipid metabolism-associated miRNA, miR-4431. We found that serum miR-4431 was significantly overexpressed in obese and type 2 diabetes mellitus individuals, and it was positively correlated with BMI and FPG. In HFD mice, increased levels of miR-4431 were present in the serum, WAT, and liver, and it was mainly expressed in the liver. Although miR-4431 had no effect on the body weight and adipose tissue weight, glucose tolerance, insulin sensitivity, and lipid levels were all disordered when miR-4431 was overexpressed. These results indicate the importance of miR-4431 in the development of type 2 diabetes mellitus.

It has been reported that a large fraction of extracellular circulating miRNAs are present in exosomes, which are the main mediators of cell-to-cell communication that coordinate biological functions[15,16]. Adipose tissue is a major source of circulating exosomal miRNAs[16]. The liver plays a major role in glucose metabolism due to its role in glucose storage and release[17]. Existing evidence implies that miRNAs can act as intermediate media between adipose tissues and the liver. For example,

Table 2 | Top 30 downstream target genes of miR-4431 predicted using TargetScan software

Target rank	Target gene	Gene name	KEGG pathway
1	UBBP4	Ubiquitin B pseudogene 4	/
2	TEX40	Testis expressed 40	/
3	WI2-3308P17.2	Uncharacterized protein	/
4	SLC4A11	solute carrier family 4, Sodium borate transporter, member 11	/
5	TRIM60	Tripartite motif containing 60	/
6	PRAMEF26	PRAME family member 26	/
7	PRAMEF11	PRAME family member 11	/
8	PRAMEF4	PRAME family member 4	/
9	AL626787.1	/	/
10	AC010336.1	Uncharacterized protein	
11	SIX3	SIX homeobox 3	/
12	FAM222B	Family with sequence similarity 222, member B	/
13	PTP4A2	Protein tyrosine phosphatase type IVA, member 2	/
14	RAB20	RAB20, member RAS oncogene family	/
15	ZNF546	Zinc finger protein 546	Herpes simplex virus 1 infection
16	ZRANB1	Zinc finger, RAN-binding domain containing 1	/
17	**TRIP10**	**Thyroid hormone receptor interactor 10**	**Insulin signaling pathway**
18	CYP46A1	Cytochrome P450, family 46, subfamily A, polypeptide 1	Primary bile acid biosynthesis
19	PITX1	Paired-like homeodomain 1	/
20	CCDC140	Coiled-coil domain containing 140	/
21	MRPL2	Mitochondrial ribosomal protein L2	/
22	RBM12B-AS1	RBM12B antisense RNA 1	/
23	AKR1C2	Aldo-keto reductase family 1, member C2	Steroid hormone biosynthesis; Chemical carcinogenesis
24	GPR139	G protein-coupled receptor 139	/
25	C19orf80	Chromosome 19 open reading frame 80	Cholesterol metabolism
26	NBPF3	Neuroblastoma breakpoint family, member 3	/
27	SH3YL1	SH3 domain containing, Ysc84-like 1 (S. cerevisiae)	/
28	NTSR1	Neurotensin receptor 1 (high affinity)	Calcium signaling pathway; Neuroactive ligand–receptor interaction
29	LY6K	Lymphocyte antigen 6 complex, locus K	/
30	CD177	CD177 molecule	/

Table 3 | Top 22 downstream target genes of miR-4431 predicted using miRDB software

Target rank	Target gene	Gene name	KEGG pathway
1	SLC4A11	Solute carrier family 4 member 11	/
2	MITD1	Microtubule interacting and trafficking domain containing 1	/
3	PRAMEF26	PRAME family member 26	/
4	SIX3	SIX homeobox 3	/
5	RNF111	Ring finger protein 111	/
6	CATSPERZ	Catsper channel auxiliary subunit zeta	/
7	PRAMEF25	PRAME family member 25	/
8	NBPF3	NBPF member 3	/
9	ZNF546	Zinc finger protein 546	/
10	PRAMEF4	PRAME family member 4	/
11	KRR1	KRR1, small subunit processome component homolog	/
12	SETD4	SET domain containing 4	/
13	CYP46A1	Cytochrome P450 family 46 subfamily A member 1	Primary bile acid biosynthesis
14	CTNNA3	Catenin alpha 3	Endometrial cancer; Adherens junction; Bacterial invasion of epithelial cells; Arrhythmogenic right ventricular cardiomyopathy (ARVC); Leukocyte transendothelial migration; Gastric cancer; Hippo signaling pathway; Herpes simplex virus 1 infection; Pathways in cancer
15	TRIM60	Tripartite motif containing 60	/
16	GPR139	G protein-coupled receptor 139	/
17	NSD2	Nuclear receptor binding SET domain protein 2	Lysine degradation; Transcriptional misregulation in cancer
18	SH3YL1	SH3 and SYLF domain containing 1	/
19	SRP19	Signal recognition particle 19	Protein export
20	AGT	Angiotensinogen	Glyoxylate and dicarboxylate metabolism; Alanine, aspartate, and glutamate metabolism; Glycine, serine, and threonine metabolism; Peroxisome; Carbon metabolism; Metabolic pathways
21	TIMP3	TIMP metallopeptidase inhibitor 3	Proteoglycans in cancer; MicroRNAs in cancer
22	**PRKD1**	**Protein kinase D1**	**Aldosterone synthesis and secretion; Rap1 signaling pathway**

extracellular vesicle-derived miR-150-5p secreted by adipose-derived mesenchymal stem cells inhibits the expression of C-X-C motif chemokine ligand 1 to attenuate hepatic fibrosis[18].

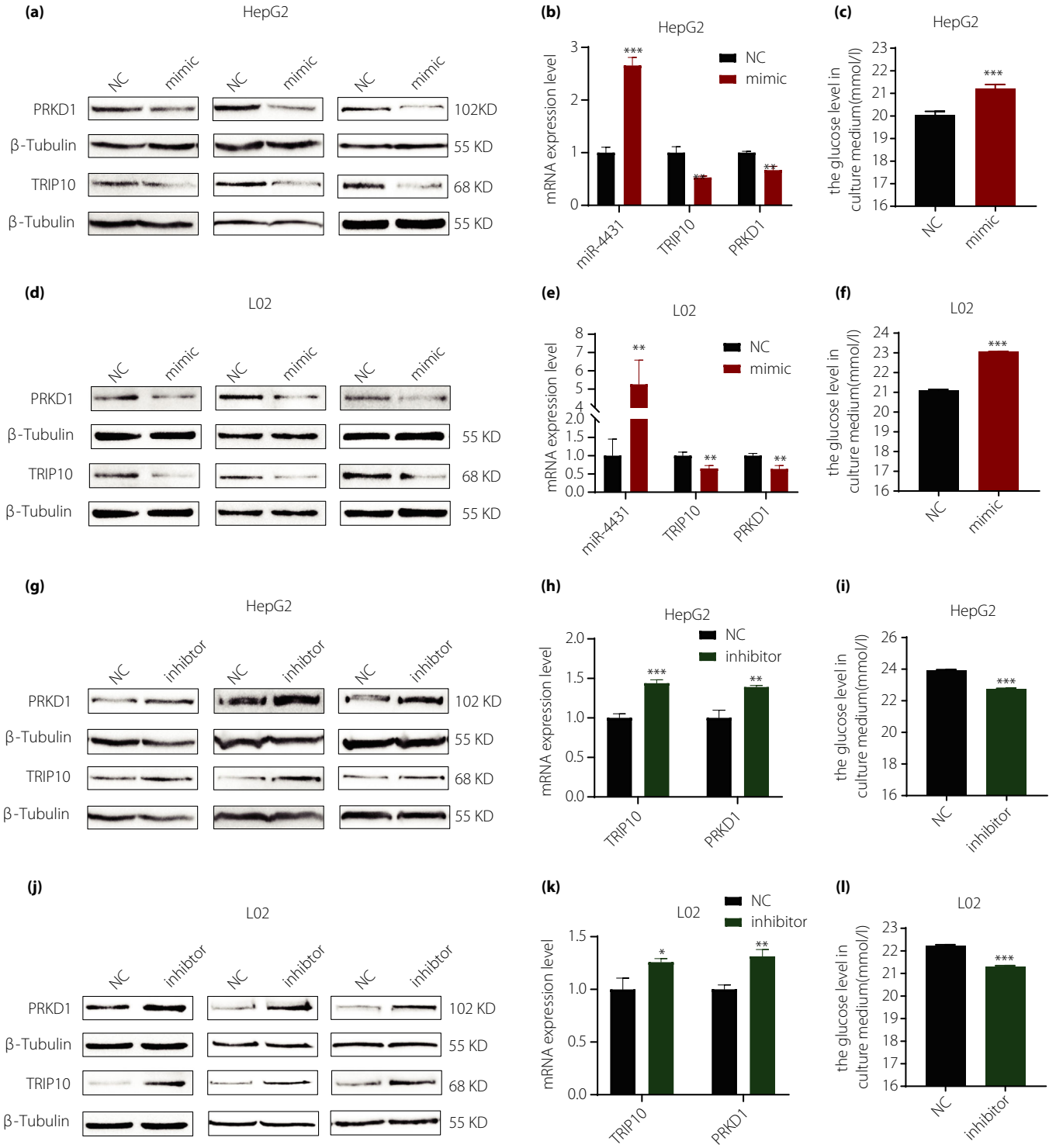

Figure 3 | Effects of miR-4431 on the expression levels of TRIP10, PRKD1, and glucose metabolism in HepG2 and L02 cells. After transfection with miR-4431 mimic for 24 h, the expression levels of TRIP10 and PRKD1 in HepG2 (a, b) and L02 (d, e) cells were detected (n = 3). Further, glucose content in the supernatant of HepG2 (c) and L02 (f) cells was determined (n = 3). After transfection with miR-4431 antisense oligonucleotide for 24 h, the expression levels of TRIP10 and PRKD1 and glucose consumption ability in HepG2 (G-I) and L02 (j–l) cells were analyzed (n = 3). t-test, $^{*}P < 0.05$, $^{**}P < 0.01$, $^{***}P < 0.001$, the difference was statistically significant.

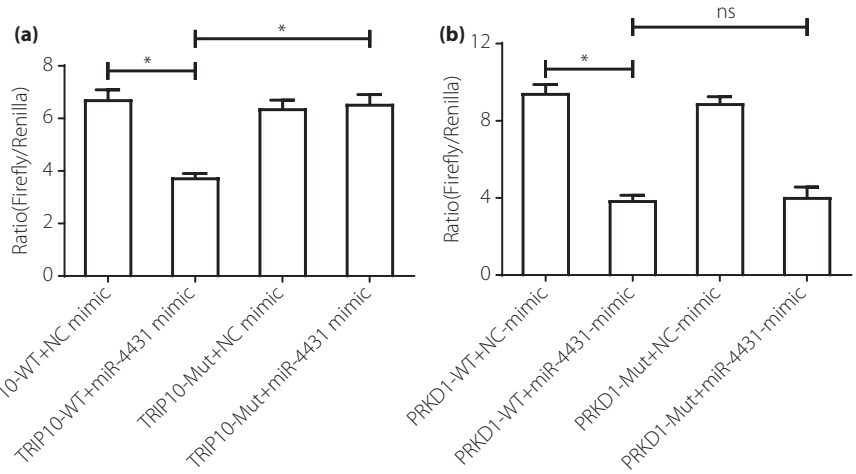

Figure 4 | Effects of miR-4431 on TRIP10 and PRKD1 3′UTR. A luciferase reporter plasmid containing the 3′UTR of TRIP10 or PRKD1 was constructed, and the luciferase activity was tested in HEK-293T cells expressing miR-4431 ($n = 3$). *t*-test, $^{*}P < 0.05$, $^{**}P < 0.01$, $^{***}P < 0.001$, the difference was statistically significant.

Besides, adipose tissue-secreted miR-99b inhibits the expression of fibroblast growth factor 21 in the liver to alter glucose metabolism[16]. Additionally, gonadal WAT-derived exosomal miR-222 represses the expression of insulin receptor substrate 1 in the liver to promote insulin resistance[19]. In this study, accompanied by an increased WAT content, HFD mice presented increased levels of miR-4431 in the serum, WAT, and liver. These findings suggest that obesity-induced elevated serum miR-4431 might originate from adipose tissue-derived exosomes, which should be elucidated further.

Next, we used TargetScan and miRDB software to predict the potential downstream genes of miR-4431 and KEGG pathway enrichment to analyze the metabolic processes of target genes. We screened out TRIP10 and PRKD1, the downstream target genes of miR-4431, to regulate glucose metabolism. Hye-Seung Jun[20] pointed out that the protein and mRNA levels of TRIP10 in visceral adipose tissues of obese mice induced by HFD significantly decreased, which may be related to an increased insulin resistance in obese mice. Furthermore, studies have reported that TRIP10 plays an important role in insulin-stimulated glucose transport[21]. Similarly, the first evidence of the role of PRKD1 in pancreatic β-cells demonstrated that PRKD1 promotes insulin secretion[22]. Additionally, the latest findings showed that the P2Y1-PRKD1 pathway contributes to a substantially greater proportion of insulin secretion from islets[23]. These results indicate that TRIP10 and PRKD1 play important roles in glucose metabolism.

Consistent with bioinformatics expectations, our results showed that HFD mice presented a remarkable reduction in mRNA expression levels of TRIP10 and PRKD1, which were overturned in the HFD + miR-4431 sponge mice. Interestingly, compared with the ND + NC mimic mice, the expression level of PRKD1 significantly increased in the ND+miR-4431 mimic mice. Previous studies have shown that TRIP10 and PRKD1 play beneficial roles in glucose metabolism[20-22] In the ND group, elevated TRIP10 and PRKD1 expression levels increased due to the presence of miR-4431 mimic, which may be a stress reaction in the body to resist abnormal glucose metabolism. Moreover, different regulation patterns probably exist under different conditions. In the HepG2 and L02 cells, miR-4431 could downregulate TRIP10 and PRKD1. The luciferase reporter assay showed that miR-4431 could bind to TRIP10 and PRKD1 3′UTR; however, unfortunately, we did not find the critical sequence in the 3′UTR of PRKD1 that is required for binding to miR-4431.

Among the predicted genes, we identified several genes, such as catenin alpha 3, nuclear receptor binding SET domain protein 2, and TIMP metallopeptidase inhibitor 3, which were associated with cancer development. Some of these gene-related tumors are obesity-associated tumors or cancers, such as hepatocellular carcinomas, prostate cancer, and breast cancer.[24-26]. Logically, we can reasonably deduce that miR-4431 might be involved in the obesity-induced occurrence of malignant tumors while its specific effects need to be further elucidated. Moreover, although KEGG pathway enrichment showed that the 10 overlapping genes could not be involved in glucose metabolism, their specific function should be fully confirmed using molecular biology technology.

Above all, this study demonstrated that serum miR-4431 levels were significantly high in obese and type 2 diabetes mellitus individuals. Moreover, miR-4431 impairs glucose metabolism both *in vivo* and *in vitro*, and TRIP10 and PRKD1 are the downstream target genes of miR-4431. In conclusion, miR-4431 targets TRIP10/PRKD1 and impairs glucose metabolism. These findings suggest that miR-4431 is a promising target for the treatment of obesity-associated metabolic syndrome.

ACKNOWLEDGMENTS

This research was funded by the Natural Science Foundation of China (grant numbers 81960152, 82160156, 81900707), Scientific and Technological Research Project of Xinjiang Production and Construction Corps (grant numbers 2018AB018 and 2021AB028), Xinjiang Production and Construction Corps Key Areas Innovation Team Project (grant number 2018CB002), and Projects of Shihezi University (grant number GJHZ201703).

DISCLOSURE

The authors declare no conflict of interest.

Approval of the research protocol: The research protocol was approved by the Medical Ethics Committee of the First Affiliated Hospital of Shihezi University School of Medicine.

Informed consent: The consent form and ethical approval were provided by the Medical Ethics Committee at the First Affiliated Hospital, Shihezi University School of Medicine (reference number 2019-029-01).

Approval date of registry and registration no. of the study/trial: N/A.

Animal studies: All procedures involving animals were performed in accordance with the guidelines established by the Medical Ethics Committee of the First Affiliated Hospital of Shihezi University School of Medicine, Xinjiang, China (reference number A2019-087-01).

REFERENCES

1. Chooi YC, Ding C, Magkos F. The epidemiology of obesity. *Metabolism* 2019; 92: 6–10.
2. Xu Y, Wang L, He J, *et al*. Prevalence and control of diabetes in Chinese adults. *JAMA* 2013; 310: 948–959.
3. Fonseca-Alaniz MH, Takada J, Alonso-Vale MI, *et al*. Adipose tissue as an endocrine organ: from theory to practice. *J Pediatr (Rio J)* 2007; 83: S192–S203.
4. Manoel Alves J, Handerson Gomes Teles R, do Valle Gomes Gatto C, *et al*. Mapping research in the obesity, adipose tissue, and microRNA field: a bibliometric analysis. *Cells* 2019; 8: 1581.
5. Xu H, Du X, Xu J, *et al*. Pancreatic beta cell microRNA-26a alleviates type 2 diabetes by improving peripheral insulin sensitivity and preserving beta cell function. *PLoS Biol* 2020; 18: e3000603.
6. Higuchi C, Nakatsuka A, Eguchi J, *et al*. Identification of circulating miR-101, miR-375 and miR-802 as biomarkers for type 2 diabetes. *Metabolism* 2015; 64: 489–497.
7. Zhang F, Ma D, Zhao W, *et al*. Obesity-induced overexpression of miR-802 impairs insulin transcription and secretion. *Nat Commun* 2020; 11: 1822.
8. Willeit P, Skroblin P, Moschen AR, *et al*. Circulating microRNA-122 is associated with the risk of new-onset metabolic syndrome and type 2 diabetes. *Diabetes* 2017; 66: 347–357.
9. Castaño C, Kalko S, Novials A, *et al*. Obesity-associated exosomal miRNAs modulate glucose and lipid metabolism in mice. *Proc Natl Acad Sci USA* 2018; 115: 12158–12163.
10. Zhu J, Wang C, Zhang X, *et al*. Correlation analysis of microribonucleic acid-155 and microribonucleic acid-29 with type 2 diabetes mellitus, and the prediction and verification of target genes. *J Diabetes Investig* 2021; 12: 165–175.
11. Zavatta G, Casadio E, Rinaldi E, *et al*. Aldosterone and type 2 diabetes mellitus. *Horm Mol Biol Clin Investig* 2016; 26: 53–59.
12. Takahashi H, Shibasaki T, Park J-H, *et al*. Role of Epac2A/Rap1 signaling in interplay between incretin and sulfonylurea in insulin secretion. *Diabetes* 2015; 64: 1262–1272.
13. La Sala L, Crestani M, Garavelli S, *et al*. Does microRNA perturbation control the mechanisms linking obesity and diabetes? Implications for cardiovascular risk. *Int J Mol Sci* 2020; 22: 143.
14. Steppan CM, Bailey ST, Bhat S, *et al*. The hormone resistin links obesity to diabetes. *Nature* 2001; 409: 307–312.
15. Vasu S, Kumano K, Darden CM, *et al*. MicroRNA signatures as future biomarkers for diagnosis of diabetes states. *Cells* 2019; 8: 1533.
16. Thomou T, Mori MA, Dreyfuss JM, *et al*. Adipose-derived circulating miRNAs regulate gene expression in other tissues. *Nature* 2017; 542: 450–455.
17. Vienberg S, Geiger J, Madsen S, *et al*. MicroRNAs in metabolism. *Acta Physiol* 2017; 219: 346–361.
18. Du Z, Wu T, Liu L, *et al*. Extracellular vesicles-derived miR-150-5p secreted by adipose-derived mesenchymal stem cells inhibits CXCL1 expression to attenuate hepatic fibrosis. *J Cell Mol Med* 2021; 25: 701–715.
19. Li D, Song H, Shuo L, *et al*. Gonadal white adipose tissue-derived exosomal miR-222 promotes obesity-associated insulin resistance. *Aging* 2020; 12: 22719–22743.
20. Jun H-S, Hwang K, Kim Y, *et al*. High-fat diet alters PP2A, TC10, and CIP4 expression in visceral adipose tissue of rats. *Obesity* 2008; 16: 1226–1231.
21. Chang L, Adams RD, Saltiel AR. The TC10-interacting protein CIP4/2 is required for insulin-stimulated Glut4 translocation in 3T3L1 adipocytes. *Proc Natl Acad Sci USA* 2002; 99: 12835–12840.
22. Sumara G, Formentini I, Collins S, *et al*. Regulation of PKD by the MAPK p38delta in insulin secretion and glucose homeostasis. *Cell* 2009; 136: 235–248.
23. Khan S, Ferdaoussi M, Bautista A, *et al*. A role for PKD1 in insulin secretion downstream of P2Y1 receptor activation in mouse and human islets. *Physiol Rep* 2019; 7: e14250.
24. He B, Li T, Guan L, *et al*. CTNNA3 is a tumor suppressor in hepatocellular carcinomas and is inhibited by miR-425. *Oncotarget* 2016; 7: 8078–8089.
25. Stangl-Kremser J, Lemberger U, Hassler MR, *et al*. The prognostic impact of tumour NSD2 expression in advanced prostate cancer. *Biomarkers* 2020; 25: 268–273.
26. Jackson HW, Hojilla CV, Weiss A, *et al*. Timp3 deficient mice show resistance to developing breast cancer. *PLoS One* 2015; 10: e0120107.

SUPPORTING INFORMATION

Additional supporting information may be found online in the Supporting Information section at the end of the article.

Table S1 | Sequence for hsa-miR-4431

Table S2 | Primer sequences of target genes

Figures S1 | Data dispersion of individuals in this study.